E6-2001-154

J.Adam[1], J.Dobeš[2], M.Honusek[2], V.G.Kalinnikov,
J.Mrázek[2], V.S.Pronskikh[3], P.Čaloun[1], N.A.Lebedev,
V.I.Stegailov, V.M.Tsoupko-Sitnikov

MEASUREMENT OF $\gamma\gamma$-COINCIDENCES AND $^{152}Tb \rightarrow {}^{152}Gd$ DECAY SCHEME

[1]On leave from Nuclear Physics Institute of ASCR, Řež, Czech Republic
[2]Nuclear Physics Institute of ASCR, Řež, Czech Republic
[3]On leave from St.Petersburg State Institute of Technology, Russia

The paper deals with continual measurements of the $\gamma\gamma$-coincidences from the ^{152}Tb $\longrightarrow$ ^{152}Gd decay. A tantalum target was irradiated by an internal proton beam (E_p=660 MeV, I_p=5$_\mu$A) of the LNP Phasotron and a radioactive source of ^{152}Tb was prepared from it by chromatographic isolation followed by electromagnetic separation. The gamma-rays were recorded by two HPGe detectors with the efficiencies ε_γ=19% (CANBERRA) and 28% (ORTEC) and the energy resolution ΔE_γ=1.8 and 1.9 keV (^{60}Co) respectively. The axes of the detectors made an angle of $\approx 100°$ and the source-to-detector distance was $\approx$ 35 mm. The detectors were protected with a Pb filter 7 mm thick placed between them to avoid registration of Compton scattered photons. The resolution time of the coincidence circuit was $\approx$ 20 ns. The coincidences were recorded event by event as the channel numbers K_i and K_j in the first and second detectors respectively and the time passed between the detection of these two pulses in the interval (0 ns - 180 ns).

After the measurements had been finished the true coincidences were selected by setting a time gate and sorting the raw data into a two-dimensional matrix. The spectra of $\gamma\gamma$-coincidences were obtained by setting gates on intensive γ-peaks followed by subtracting the Compton distribution spectra from the resulting ones. The number of events was increased by a factor of two by summing each pair of the gate spectra from the X and Y detectors corresponding to the same γ-energy. Before summing up, these spectra were corrected channel by channel for non-linearity of the detectors' electric circuits. The number of the $\gamma\gamma$-coincidences acquired in a spectrum by gating a peak with $E_{nj}(\gamma)$ for the X detector $S^{\bar{X},Y}_{\gamma\gamma}(E_{nj}(\gamma), E_{im}(\gamma))$ is

$$S^{\bar{X},Y}_{\gamma\gamma}(E_{nj}(\gamma), E_{im}(\gamma)) = \varepsilon^X_\gamma(E_{nj}(\gamma)) I_\gamma(E_{nj}(\gamma)) \varepsilon^Y_\gamma(E_{im}(\gamma)) \times \\ \times I_\gamma(E_{im}(\gamma)) R_{ji} N T W(\Theta) \quad (1)$$

where indices n, j, i, m are the numbers of the excited states between which the transition occurs, N is the number of nuclei decayed per second, T is the coincidence measurement time, R_{ij} is the branching coefficient, $\varepsilon^X_\gamma, \varepsilon^Y_\gamma$ is the absolute recording efficiency of the X and Y detectors for γ-quanta with E_γ, $W(\Theta)$ is the angular correlation

coefficient of the coinciding γ-quanta. Analogously, for the Y detector we have :

$$S_{\gamma\gamma}^{X,\bar{Y}}(E_{im}(\gamma), E_{nj}(\gamma)) = \varepsilon_{\gamma}^{Y}(E_{nj}(\gamma)) I_{\gamma}(E_{nj}(\gamma)) \varepsilon_{\gamma}^{X}(E_{im}(\gamma)) \times \\ \times I_{\gamma}(E_{im}(\gamma)) R_{ji} NTW(\Theta). \quad (2)$$

Thus, the total number of coincidence events in both detectors for a pair of coincident γ-quanta is

$$S_{\gamma\gamma}^{\bar{X},\bar{Y}}(E_{im}(\gamma), E_{nj}(\gamma)) = S_{\gamma\gamma}^{\bar{X},Y}(E_{nj}(\gamma), E_{im}(\gamma)) + S_{\gamma\gamma}^{X,\bar{Y}}(E_{im}(\gamma), E_{nj}(\gamma)). \quad (3)$$

Recording $\gamma\gamma$-coincidences we simultaneously recorded single γ-spectra with the same two detectors. The number of γ-quanta recorded in the X and Y spectra is :

$$S_{\gamma}^{X}(E_{nj}(\gamma)) = \varepsilon_{\gamma}^{X}(E_{nj}(\gamma)) I_{\gamma}(E_{nj}(\gamma)) NT \quad (4)$$

or

$$S_{\gamma}^{Y}(E_{nj}(\gamma)) = \varepsilon_{\gamma}^{Y}(E_{nj}(\gamma)) I_{\gamma}(E_{nj}(\gamma)) NT. \quad (5)$$

Using the above relations one can calculate the branching ratio from the experimental data :

$$(R_{ji})_{exp} = \frac{S_{\gamma\gamma}^{\bar{X},\bar{Y}}(E_{im}(\gamma), E_{nj}(\gamma)) [W(\Theta)]^{-1}}{S_{\gamma}^{X}(E_{nj}(\gamma)) S_{\gamma}^{Y}(E_{im}(\gamma)) + S_{\gamma}^{X}(E_{im}(\gamma)) S_{\gamma}^{Y}(E_{nj}(\gamma))} \times NT. \quad (6)$$

We found it convenient to compare the experimental branching coefficient ratio $(R_{ji}/R_{22})_{exp}$ to the calculated one $(R_{ji}/R_{22})_{calc}$ which had been deduced from the proposed decay scheme and placement of the γ-transitions.

$$(R_{ji})_{calc} = s_i D_{ji} \qquad \text{where} \quad (7)$$

$$s_i = \frac{1}{\sum_{x=1}^{i-1} I_{ix}} \qquad \text{and} \qquad d_{ix} = s_i I_{ix} \quad (8)$$

where I_{ix} is the total γ-transition intensity, and the branching coefficient D_{ji} is deduced from the relation :

$$D_{ji} = d_{ji} + \sum_{z_1>i}^{j-1} d_{jz_1} d_{z_1 i} + \\ + \sum_{z_{\eta-1}>z_{\eta-2}}^{j-1} \sum_{z_{\eta-2}>z_{\eta-3}}^{j-2} \cdots \sum_{z_1>i}^{j-(\eta-1)} d_{jz_{\eta-1}} d_{z_{\eta-1}z_{\eta-2}} \cdots d_{z_1 i} + \\ + d_{i\,i-1} d_{i-1\,i-2} \cdots d_{j+2\,j+1} d_{j+1\,j} \,. \quad (9)$$

A number of coefficients R_{ji} calculated by the program COIN [1] for the ^{152}Gd decay scheme are shown in Table 1.

Now let us consider the angular correlation coefficient in our experimental conditions. It can be written as follows :

$$W(\Theta) = 1 + Q_{22} A_{22} P_2(\cos(\Theta)) + Q_{44} A_{44} P_4(\cos(\Theta)) \quad (10)$$

$$Q_{22} = Q_2(Det\ X) Q_2(Det\ Y)$$

$$Q_{44} = Q_4(Det\ X) Q_4(Det\ Y) \quad (11)$$

where Q_{22} and Q_{44} are the attenuation coefficients taking into account the finite size of the detectors. We calculated Q_2 and Q_4 for the X (CANBERRA) and Y (ORTEC) detectors for a number of energies (d=35mm) by the method of Krane [2] using the program SAC [3] (Table 2).

Thus, assuming the average values $Q_{22} = 0.4686$ and $Q_{44} = 0.0224$ take the angular correlation coefficient in the form :

$$W(100^\circ) = 1 - 0.2131 A_{22} + 0.00596 A_{44} \,. \quad (12)$$

When calculating $W(100^\circ)$ for the transition $I^\pi - (L) \to 2^+ - (2) \to 0^+$ we used the A_{22} and A_{44} from [4], see Table 3. The values of $(R_{22})_{exp}$ were calculated without taking into account angular correlation between gamma-rays with energy E_{i2} and E_{21} ($W_{i2,21}(100^\circ) = 1$). Then the average $(R_{22})_{exp} = 0.895(26)$ with $\chi^2 = 87.7$. After that we corrected them for angular correlation dividing $(R_{22})_{exp}$ by $W_{i2,21}(100^\circ)$, then the average $(R_{22})_{exp}/W_{i2,21}(100^\circ) = 0.875(24)$ with $\chi^2 = 68.1$.

When the multipolarity of transitions or/and spin of levels are uncertain we choose from possible set their values such ones which give ratio $(R_{22})_{exp}/W_{i2,21}(100°)$ closer to unity. The values of $(R_{22})_{exp}$ and $(R_{22})_{exp}/W(100°)$ for the transitions $I^{\pi}(L) \to 2^{+}(2) \to 0^{+}$ are shown in Figure 1. I^{π} is the spin and parity of the initial level. These R_{22} should be the same for each shown transition, therefore in several cases they differ significantly from each other, sometimes by 2σ. This fact could be explained as a result of the cascade transition intensity weakening which has not been taken into account with (6). It also appears if one calculates the ratio of the detector recording efficiencies, as shown in Figure 2. Although the discrepance in R_{22} values somewhat decreased, finally good agreement was not reached. Probably, the too low R_{22} in case of 271 keV and 411 keV can be explained by dependence of the coincidence efficiency on the γ-quanta energy. Our experimental conditions therefore do not allow fully quantitative estimation of such dependence.

Those γ-quanta close in energy which cannot be resolved in single γ-spectra (due to limited energy resolution of the detectors) can however turn up in $\gamma\gamma$-coincidence spectra. When intensities of components of double and triple peaks are being determined, an additional uncertainity often arises from an indefinite angular correlation correction factor of the coincident γ-quanta. Analysis of the transitions that fed the first excited state in ^{152}Gd gave that factor about $\pm 20\%$ of their average intensity. It appeared that different single γ-transitions feeding the same level have nearly equal values of the experimental coincidence intensity ratios $\frac{S_{\gamma\gamma}(E_{if},E_{f2})}{S_{\gamma\gamma}(E_{if},E_{21})}$. The mean values of such ratios are shown in Table 4.

We used these ratios to split intensities of the double and triple γ-lines into individual ones, because we are able to estimate experimentally only $S_{\gamma\gamma}(E_{if}, E_{f2})_{exp}$, $S_{\gamma\gamma}(E_{i'f'}, E_{f'2})_{exp}$ and the sum $\{S_{\gamma\gamma}(E_{if}, E_{21}) + S_{\gamma\gamma}(E_{i'f'}, E_{21})\}_{exp}$ Let us introduce this ratio :

$$C(E_{f2}, E_{21}) \equiv \left\{ \frac{S_{\gamma\gamma}(E_{if}, E_{f2})}{S_{\gamma\gamma}(E_{if}, E_{21})} \right\}_{avg} . \qquad (13)$$

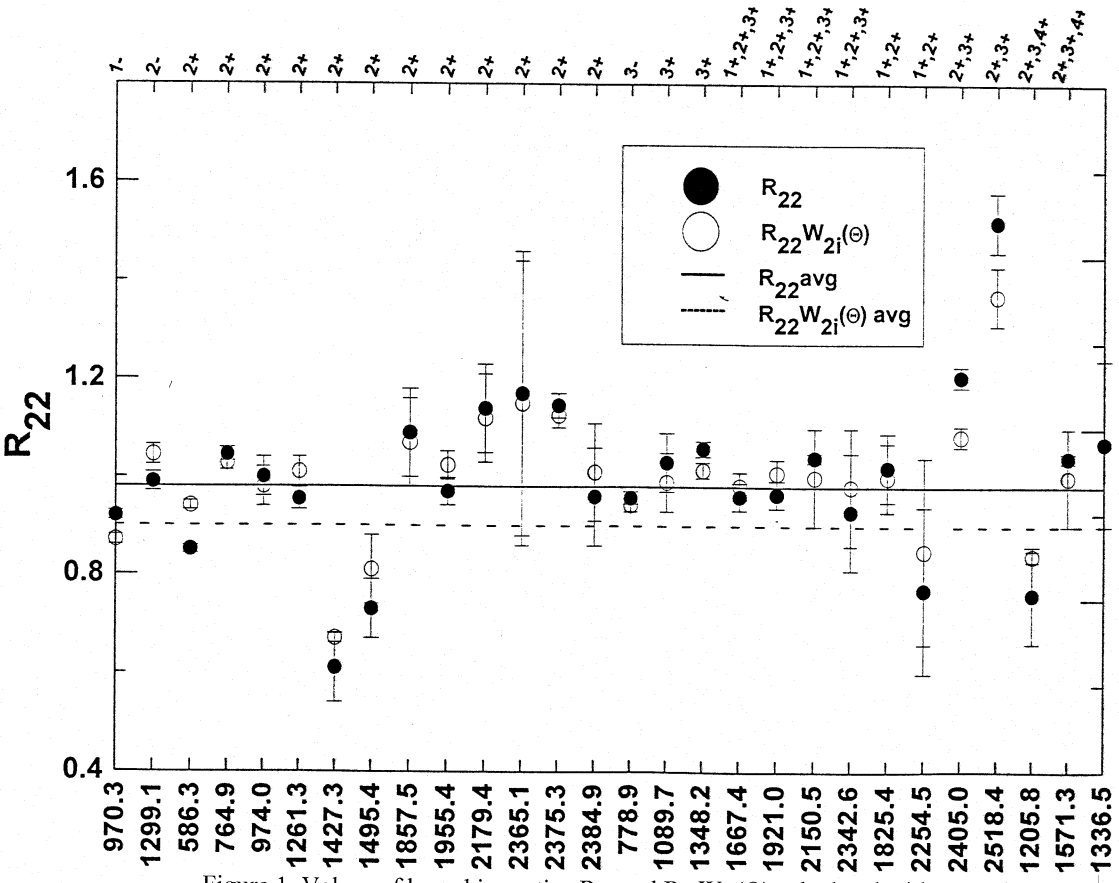

Figure 1. Values of branching ratios R_{22} and $R_{22}W_{2i}(\Theta)$ calculated without and with taking into account angular correlations of γ-quanta coupling the first excited state.

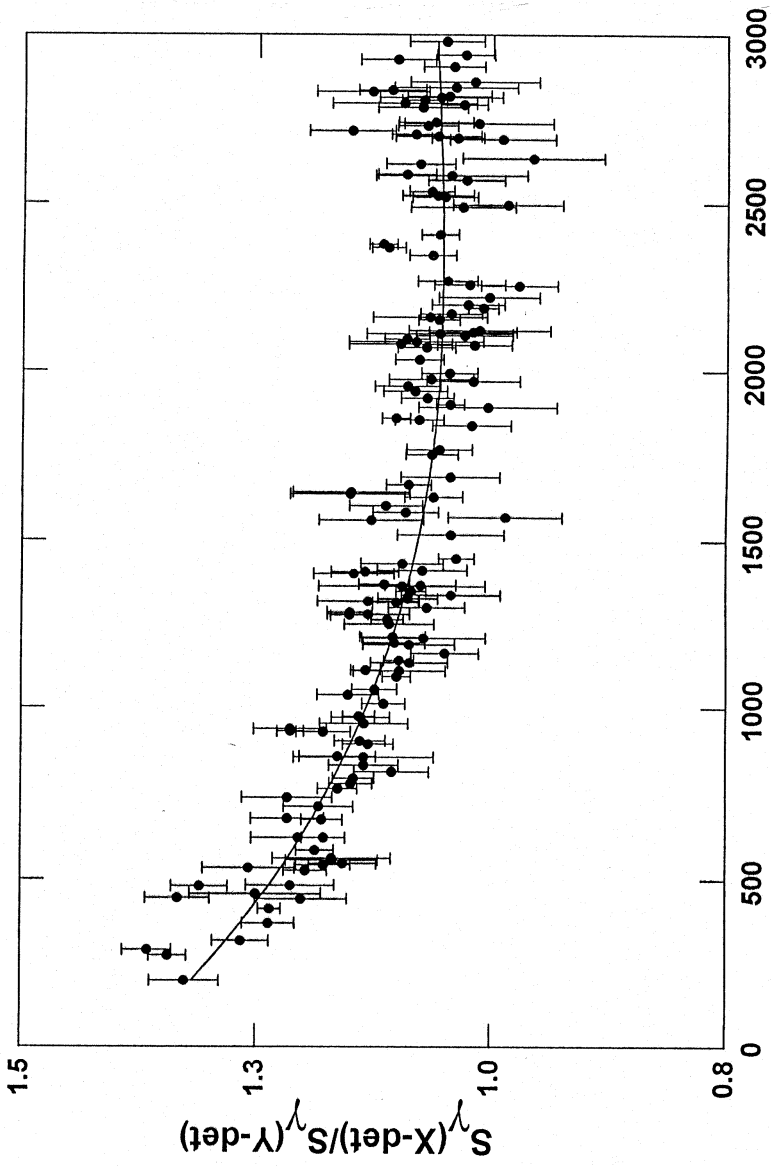

Figure 2. Ratios of peak areas with given energy E_γ registered in X- and Y-detectors.

As (13) was written for single averaged transitions E_{if}, for a double one we can write :

$$A_{exp}(E_{if}, E_{f2}) \equiv \left\{ \frac{S_{\gamma\gamma}(E_{if}, E_{f2})}{S_{\gamma\gamma}(E_{if}, E_{21}) + S_{\gamma\gamma}(E_{i'f'}, E_{21})} \right\}_{exp}, \tag{14}$$

$$A_{exp}(E_{i'f'}, E_{f'2}) \equiv \left\{ \frac{S_{\gamma\gamma}(E_{i'f'}, E_{f'2})}{S_{\gamma\gamma}(E_{if}, E_{21}) + S_{\gamma\gamma}(E_{i'f'}, E_{21})} \right\}_{exp}. \tag{15}$$

Thus, intensities of components of a doublet E_{if} and $E_{i'f'}$ can be derived from the relations :

$$\frac{A_{exp}(E_{if}, E_{f2})}{C(E_{f2}, E_{21})} = \frac{I_\gamma(E_{if})}{I_\gamma(E_{if} \approx E_{i'f'})}, \tag{16}$$

$$\frac{A_{exp}(E_{i'f'}, E_{f'2})}{C(E_{f'2}, E_{21})} = \frac{I_\gamma(E_{i'f'})}{I_\gamma(E_{if} \approx E_{i'f'})}. \tag{17}$$

where the doublet γ-transition intensity is $I_\gamma(E_{if} \approx E_{i'f'}) = I_\gamma(E_{if}) + I_\gamma(E_{i'f'})$. Similarly, we also calculated components of the triplets.

The coincidence intensity ratio in case using the whole coincidence matrix (summing of X and Y spectra) can be calculated by the equation :

$$\frac{S^{\bar{X}\bar{Y}}_{\gamma\gamma}(E_{if}, E_{f2})}{S^{\bar{X}\bar{Y}}_{\gamma\gamma}(E_{if}, E_{21})} = \frac{S^X_\gamma(E_{f2}) \left\{ \frac{\varepsilon^Y_\gamma(E_{f2})}{\varepsilon^X_\gamma(E_{f2})} + \frac{\varepsilon^Y_\gamma(E_{if})}{\varepsilon^X_\gamma(E_{if})} \right\} R_{ff} W_\gamma(E_{if}, E_{f2})}{S^X_\gamma(E_{21}) \left\{ \frac{\varepsilon^Y_\gamma(E_{21})}{\varepsilon^X_\gamma(E_{21})} + \frac{\varepsilon^Y_\gamma(E_{if})}{\varepsilon^X_\gamma(E_{if})} \right\} R_{f2} W_\gamma(E_{if}, E_{21})} \cdot \tag{18}$$

Here we assumed the ratio

$$W_\gamma(E_{if}, E_{f2})/W_\gamma(E_{if}, E_{21}) \approx W_\gamma(E_{i'f'}, E_{f2})/W_\gamma(E_{i'f'}, E_{21}).$$

It is clear that $A_{22}P_2(\cos 100°)$ differs from $A_{44}P_4(\cos 100°)$ by a factor of 3 (see Table 3) or less, but since Q_{44} is approximately 28 times smaller than Q_{22}, one can neglect the term $Q_{44}A_{44}P_4(\cos 100°)$.

Thus when calculating intensities of components of the double peaks from the coincidence intensity ratios (as given above), we found that

the angular correlation factor (19) does not depend on the spin and parity of the i-th level and the multipolarity of the upper γ-transition (L_{if}, L'_{if}) :

$$\frac{W(E_{if}, E_{f2}) - 1}{W(E_{if}, E_{21}) - 1} = \frac{A_2(L_{if}L'_{if}\mathrm{I}_i\mathrm{I}_f)}{A_2(L_{if}L'_{if}\mathrm{I}_i\mathrm{I}_f)} \cdot \frac{A_2(L_{f2}L'_{f2}2\mathrm{I}_f)}{U_2(\mathrm{I}_f2)A_2(2202)} =$$

$$= \frac{A_2(L_{f2}L'_{f2}2\mathrm{I}_f)}{U_2(\mathrm{I}_f2)A_2(2202)} = \frac{W(E_{i'f}, E_{f2}) - 1}{W(E_{i'f}, E_{21}) - 1} \quad (19)$$

where $U_2(\mathrm{I}_f2)$ is a factor referring to an unobserved transition E_{I_f2}.

Intensities of double and triple γ-transitions resolved by the $\gamma\gamma$-coincidences are shown in Table 5. We found 19 double transitions (13 for the first time) and 3 new triple transitions. We consider the transition of 1598 keV, identified in [5] as a double one, to be single since no coincidences of its second component with either γ970 or γ1314 was observed.

Measuring the β^+/EC decay of neutron-deficient nuclei like ^{152}Tb one can also observe annihilation quanta following positron emission. The intensity of coincidences with such quanta $S^{\bar{X},\bar{Y}}_{511,\gamma}$ has the general form (similar to (6)) :

$$\frac{S^{\bar{X},\bar{Y}}_{511,\gamma}(511(\gamma), E_{LK}(\gamma))}{[S^X_\gamma(511)S^Y_\gamma(E_{LK}) + S^Y_\gamma(511)S^X_\gamma(E_{LK})]} \left[\frac{I_\gamma(511)}{NT}\right]^{-1} = \sum_{i=L}^{M} R_{iL}I_\beta(i) \quad (20)$$

where $I_\beta(i)$ is the intensity of the β transition to the i-th level, R_{iL} is the branching coefficient calculated by (7), (8) and (9). The intensity of such a transition is expressed by (20), at first for the highest level excited in the decay and consecutively downward to the first (lowest) one. Intensities of the β^+ transitions (or their upper limits) found (see Table 6) for level energies up to 2300 keV.

Experimental ratios of electron capture to positron emission intensities are compared to the theoretical ratios for allowed unhindered (au) and unique first forbidden (1^*h) β-transitions, see Figure 3. In the general case we do not know the real annihilation quantum recording

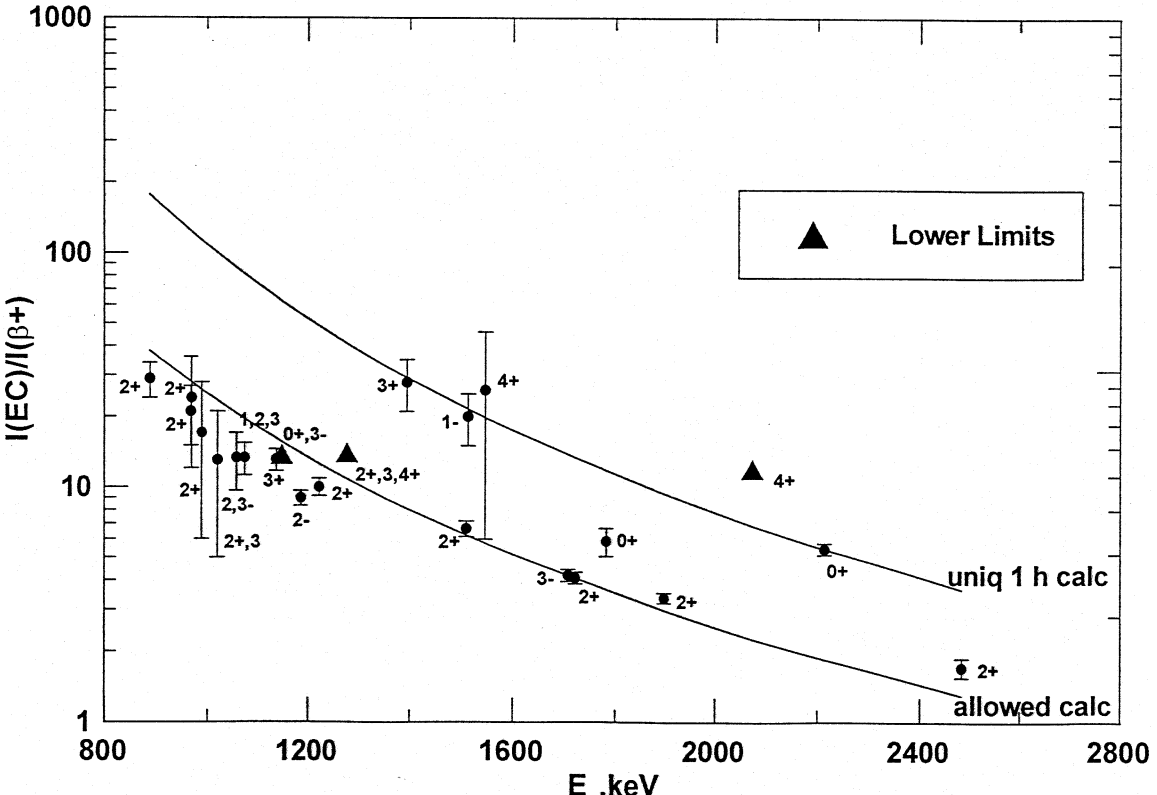

Figure 3. Experimental (points) and calculated (curves) ratios of K-electron capture to positron decay intensities for ground and excited states.

efficiencies, but we can determine $\frac{I(EC)}{I(\beta)}$ in relative units first, neglecting the efficiencies, and correct them by the normalizing coefficient. To deduce this normalizing coefficient we assume that this experimental ratio for allowed transitions is equal to the theoretical one (within approx 10% errors, see [7], [6] and Figure 27 therein). We used the allowed transition to the 3^- final state for such normalization. In accordance with Table XXI from [6], for some nuclei the ratio analysed in the case of allowed transitions almost does not differ from that of 1-st forbidden nonunique ones (within the error limits) while for others it may differ by up to 30%. Our case is the former.

In this experiment we set 91 gates on each of the two detectors, X (CANBERRA) and Y (ORTEC), embracing 116 γ-peaks (19 transitions were found to be double and 3 triple), and gained 91 coincidence spectra for each detector. The spectra corresponding to the same γ-energies were corrected for non-linearity as explained above and then summed. For each 91 resulting spectra $S_{\gamma\gamma}^{\bar{X},\bar{Y}}$ and $\sigma(S_{\gamma\gamma}^{\bar{X},\bar{Y}})$ were found and $(R_{ji})_{exp}$ calculated by (6) with $W(\Theta) = 1$.

At the first stage of analysis we thoroughly checked the results of $\gamma\gamma$-coincidence analysis performed in [5]. The direct transitions which fed the ^{152}Gd ground state were unambiquously confirmed by the $\gamma\gamma$-coincidences with the upper transition gated as shown in Table 8.

Coincidences of the transitions choosen as gates with the lower transitions proved placements of the following transitions : 271.09, 411.1165, 526.85, 543.58, 586.27, 622.79, 675.01, 703.39, 764.89, 778.9045, 794.73, 909.15, 970.32, 974.05, 990.19, 1052.15, 1137.56, 1159.82, 1190.44, 1209.03, 1299.140, 1325.86, 1348.15, 1586.22, 1631.42, 1739.46, 1757.42, 1841.15, 1857.48, 2033.89 and 2251.41 keV. For the first time placement of the transitions in Table 7 is proved by coincidences.

Part of the $\gamma\gamma$-coincidence results is given in Table 9. We determined the experimental ratio $(R_{ji}/R_{22})_{exp}$ (see equation (6)) for transitions which coincide with the most intense transitions deexciting the low energy levels. The experimental ratios were compared with the calculated ones (see Table 1) and the qualifying transitions were then placed in the decay scheme. The first and second number in the last

column of Table 9 indicates from which initial to final level the transition proceeds. The decay scheme in a tabular form is shown in Table 10.

Introduction of new excited levels was based on the results of the $\gamma\gamma$- coincidences. Obviously, energies and multipolarities of the transitions placed between the levels with known energies, spins and parities follow some rules, namely, energy balance, balance of total transition intensities and momentum and parity conservation law. Zolnowski et al. [5] introduced 41 levels on the basis of the $\gamma\gamma$-coincidences and 25 more levels were introduced tentatively on the basis of energy balance. Our measurements of $\gamma\gamma$-coincidences confirmed 40 levels, and only the 3411.5 keV level was not confirmed. Out of all the tentatively introduced levels [5] four levels at 1771.557, 1975.67, 2264.83 and 2932.66 keV agree with our $\gamma\gamma$-coincidence results. Based on the $\gamma\gamma$-coincidences we introduced 46 new levels, see Table 10. Using the conservation laws we found unique or possible spins and parities for all levels. Placement of 58 transitions on the basis of $\gamma\gamma$-coincidences and 53 transitions on the basis of mere energy balance [5] was confirmed by our $\gamma\gamma$-coincidences. In addition, we placed 131 transitions on the basis of coincidences for the first time. Thus, 242 gamma-transitions have been unambiguously (on the basis of $\gamma\gamma$-coincidences) placed in the ^{152}Tb$\rightarrow^{152}$Gd decay scheme, see Table 10. The $\log ft$ values listed there were calculated using the ^{152}Tb half-life of $17.5(1)h$, decay energy $Q_\beta = 3990(40)$ keV [8] and intensities of the ^{152}Gd level population. For some levels their intensity balances turned out to be negative and the condition $|I_{\beta i}| < \sigma(I_{\beta i})$ was satisfied. In those cases we gave only lower limits of $\log ft$ calculated on the assumption that $I'_{\beta i} = I_{\beta i} + 2\sigma(I_{\beta i})$.

J.D. acknowledges support from GACR Grant No. 202/99/0149.

V.S.P. wants to thank Prof. N.Severijns and his colleages for fruitful discussions and kind hospitality during his visit to Katholieke Universiteit Leuven, Belgium.

Table 1. Part of ratio R_{ji}s calculated by the program COIN. Absolute (upp. r) R_{ji} and ratio R_{ji}/R_{22} are given in cells. Numbers of ^{152}Gd excited levels are given in squares.

	$E_{lev}[keV]$									
R_{ji}	344	615	755	930	1047	1109	1123	1282	1314	1318
R_{ji}/R_{22}	[2]	[3]	[4]	[5]	[6]	[7]	[8]	[9]	[10]	[11]
$E_{lev}[keV]$										
344	1.754	1.754	1.754	1.754	1.754	1.754	1.754	1.754	1.754	1.754
[2]	1.00	1.00	1.00	1.00	1.00	1.00	1.00	1.00	1.00	1.00
615		13.29		1.117		0.593		0.529		0.121
[3]		7.577		0.637		0.338		0.301		0.069
755			27.85				1.621	14.66		0.167
[4]			15.79				0.924	8.358		0.095
930				11.08				5.250		1.161
[5]				6.317				2.996		0.662
1047					46.04					
[6]					26.25					
1109						37.25				0.244
[7]						21.24				0.139
1123							18.56			1.914
[8]							10.58			1.091
1282								230.8		
[9]								131.6		
1314									122.7	
[10]									69.95	
1318										28.7
[11]										16.4

Table 2. Angular correlation attenuation coefficients. X – HPGe detector (CANBERRA), Y – HPGe detector (ORTEC).

	E_γ=270 keV	E_γ=340 keV	E_γ=1500 keV
Q_2(X)	0.7035	0.7077	0.7122
Q_2(Y)	0.6562	0.6621	0.6682
Q_{22}	0.4616	0.4686	0.4759
Q_4(X)	0.1923	0.2018	0.2122
Q_4(Y)	0.0981	0.1105	0.1238
Q_{44}	0.0189	0.0223	0.0263

Table 3. Angular correlation coefficients $W(100°)$.

I_i(L)$I_{f'}$(L)I_f	A_{22}	A_{44}	$W(100°)$
0(2)2(2)0	0.3571	1.143	0.931
1(1)2(2)0	-0.25	0.0	1.053
1($\delta = +1$)2(2)0	-0.5949	-0.3809	1.124
1(2)2(2)0	0.1786	-0.7619	0.957
2(1)2(2)0	0.25	0.0	0.947
2($\delta = -1$)2(2)0	0.4527	0.1632	0.904
2(2)2(2)0	-0.0765	0.3265	1.018
3(1)2(2)0	-0.0714	0.0	1.015
3($\delta = -1$)2(2)0	-0.5290	-0.0408	1.112
3(2)2(2)0	-0.2041	-0.0816	1.043
4(2)2(2)0	0.1020	0.0091	0.978

Table 4. Average experimental coincidence intensity ratios $C(E_{f2},E_{21})$ for a number of transition pairs.

Level			Transition		Ratio
f	E_f, keV	I_f	E_{f2}, keV	$XL(E_{f2})$	$C(E_{f2},E_{21})$
3	615.373	0^+	271.09	E2	1.11(3)
4	755.395	4^+	411.1165	E2	0.92(6)
5	930.550	2^+	568.27	(E0,M1,E2)	0.61(4)
6	1047.774	0^+	703.494	E2	0.49(3)
7	1109.193	2^+	764.89	E2	0.48(3)
8	1123.183	3^-	778.9045	E1	0.48(3)
12	1314.635	1^-	970.32	E1	0.34(4)
13	1318.349	2^+	974.05	(E0,M1,E2)	0.32(4)
14	1434.017	3^+	1089.737	M1,E2	0.24(4)

Table 5. Intensities of double and triple γ-transitions resolved by $\gamma\gamma$-coincidences.

E_γ, keV	E_i	E_f	(E_{if})(calc)	$I_\gamma(\Delta I_\gamma)$
I_γ^{peak}	keV	keV	keV	(components)
557.67(7)	1605.584	1047.774	557.810	11.4(11)
17.5(5)	1839.70	1282.267	557.433	6.1(12)
703.39(7)	1047.774	344.280	703.494	237(7)
371(7)	1318.349	615.373	702.976	134(5)
814.38(16)	1861.897	1047.774	814.123	3.8(7)
5.5(5)	2729.165	1915.69	813.475	1.7(8)
818.25(8)	1941.157	1123.183	817.974	15.0(25)
16.0(4)	2133.39	1314.635	818.755	1.0(4)
855.00(9)	1470.61	615.373	855.237	3.6(7)
10.3(12)	1785.24	930.550	854.690	4.1(8)
	2169.58	1314.635	854.945	2.6(7)
1083.96(10)	1839.70	755.395	1084.305	7.0(16)
12.2(5)	2401.49	1318.349	1083.141	5.2(12)
1202.64(9)	2133.39	930.550	1202.840	4.3(12)
8.92(29)	2325.82	1123.183	1202.64	4.6(10)
1314.66(9)	1314.635	0	1314.635	186(7)
222(5)	2437.44	1123.183	1314.257	36(5)

1400.60(7)	2523.80	1123.183	1400.617	15.4(13)
24.4(5)	2719.67	1318.349	1401.321	9.0(8)
1411.48(9)	1755.76	344.280	1411.48	68(4)
101(3)	2729.165	1318.349	1410.816	33(2)
1446.43(7)	2201.73	755.395	1446.335	13.1(13)
38.7(8)	2880.652	1434.017	1446.635	25.6(26)
1517.78(7)	1862.06	344.280	1517.780	80(6)
102.5(21)	2133.39	615.373	1518.017	5.0(10)
	2641.56	1123.183	1518.377	17.5(13)
1596.75(7)	1941.157	344.280	1596.877	47.8(25)
72.1(15)	2719.67	1123.183	1596.487	24.3(18)
1605.72(7)	1605.584	0	1605.584	35(5)
58.5(11)	2729.165	1123.183	1605.982	23.5(30)
1631.42(8)	1975.67	344.280	1631.390	10.9(8)
36.1(8)	2246.772	615.373	1631.399	25.2(15)
1789.20(8)	2133.39	344.280	1789.110	75.5(20)
89.9(17)	2719.67	930.550	1789.120	14.4(11)
1841.15(9)	2772.36	930.550	1841.810	4.1(5)
12.3(3)	2964.33	1123.183	1841.147	8.2(10)
1902.45(8)	2246.772	344.280	1902.492	266(6)
268(5)	3012.06	1109.193	1902.867	2.1(4)
2043.65(10)	2386.95	344.280	2042.670	11.0(8)
15.6(4)	3152.98	1109.193	2043.787	3.0(4)
	3358.26	1314.635	2043.625	1.6(4)
2093.51(8)	2437.44	344.280	2093.160	21.1(18)
33.3(7)	2709.42	615.373	2094.047	12.2(11)
2103.54(9)	2447.96	344.280	2103.680	4.7(10)
10.11(26)	2719.67	615.373	2104.297	5.4(12)
2169.16(9)	2513.9	344.280	2169.620	6.4(18)
14.6(3)	3098.99	930.550	2168.440	8.2(20)

Table 6. Relative intensities of β^+-transitions to the levels up to 2300 keV.

i_{LEV}	I^π	E_{LEV}	I_β(i)	i_{LEV}	I^π	E_{LEV}	I_β(i)
2	2^+	344.280	118901(11200)	24	2^+	1771.557	394(110)
3	0^+	615.373	19026(1084)	25	2^+	1785.24	285(39)
4	4^+	755.395	-94(253)	26		1807.53	<62
5	2^+	930.550	35900(1967)	27		1808.95	427(126)
6	0^+	1047.774	3623(500)	28	2^+	1839.70	542(144)
7	2^+	1109.193	10865(560)	29	2^+	1861.897	<370
8	3^-	1123.183	6047(356)	30	2^+	1862.06	697(100)
9		1227.37	<314	31		1915.19	<73
10		1274.2	<114	32		1915.69	<66
11	4^+	1282.267	134(100)	33	2^+	1941.157	2062(400)
12	1^-	1314.635	467(96)	34		1975.67	<77
13	2^+	1318.349	7639(969)	35		2011.65	<192
14	3^+	1434.017	408(102)	36		2120.96	<16
15	2^+	1470.61	842(69)	37		2133.39	<104
16		1533.91	<183	38		2169.58	<17
17		1550.15	<378	39	2^+	2201.73	<32
18	2^+	1605.584	4078(680)	40	2^+	2246.772	<453
19	2^-	1643.427	3168(231)	41		2258.14	<9
20		1680.76	<187	42		2264.83	<3
21	3^+	1692.42	776(79)	43		2265.28	<4
22		1734.44	<20	44		2267.71	<5
23		1755.73	441(71)	45	2^+	2299.636	<56

Table 7. Direct transitions to the ^{152}Gd ground state confirmed by $\gamma\gamma$-coincidences.

Direct transition, keV	Gate, keV
1318.24	622.79
930.58	675.01, 909.15, 2033.89
1109.20	1190.44
1314.66	1209.03
344.2785	2405.00, 2518.42

Table 8. Transitions placed by [5] on the basis of energy balance and proved by coincidences in this work.

Gate E_{gate},keV	Initial E_i, keV	Final E_f, keV
738.69	1862.06	1123.183
1036.74	2729.165	1692.42
1089.737	1434.017	344.280
1205.83	1550.15	344.280
1495.44	1839.70	344.280
1667.38	2011.65	344.280
1789.20	2719.67	930.550
1970.49	3285.12	1314.635
2405.00	2749.20	344.280
2518.42	2862.64	344.280

Table 9. Ratios $(\frac{R_{ij}}{R_{22}})_{exp}$ from $\gamma\gamma$-coincidences.

Eg(coinc)	$\frac{R_{exp}(\Delta R_{exp})}{R_{22}}$						i	f
	344.279 (2,1)	271.094 (3,2)	411.116 (4,2)	586.272 (5,2)	764.887 (7,2)	778.904 (8,2)		
117.25				0.69(16)			6	5
175.14			11.0(11)				5	4
195.17	0.471(14)		0.46(7)			6.37(17)	13	8
209.14					15.1(21)		13	7
248.75	0.43(5)							
g 271.09	0.630(7)*						3	2
315.16	0.577(17)	3.24(9)					5	3
324.90					12.0(23)		14	7
335.56 en	0.67(14)						33	18

g 344.2785		0.625(13)	0.732(12)	0.851(8)*	1.046(14)*	0.958(13)*	2	1
351.73	0.53(3)	0.19(3)		4.74(20)			11	5
353.78 en	0.71(24)		10.5(20)				7	4
367.80	0.729(24)		12.6(3)				8	4
387.80	0.474(18)	0.345(14)		4.16(15)			13	5
g 411.1165	0.729(9)*						4	2
441.02					10.4(7)		17	7
471.98 n			15(3)				9	4
482.34	0.72(13)					10.8(11)	18	8
490.66	0.98(17)							
493.81	0.73(6)	3.9(3)					7	3
496.37	0.40(5)				10.1(7)		18	7
503.43	0.67(8)			4.0(10)			14	5
520.30	0.66(11)					11.0(10)	19	8
g 526.85	0.720(21)*		12.41(26)*				11	4
534.21 n	0.39(7)				10.1(14)		19	7
g 543.58	0.83(4)*	0.83(8)*		1.40(17)			29	13
547.47	0.64(12)		1.6(4)				30	12
g 557.67 d	0.66(6)*	0.81(12)*	1.76(16)*	0.87(9)*			18	6
d							28	11
562.98	0.62(9)		12.0(10)				13	4
579.63	2.6(9)		8.6(17)				29	11
g 586.27	0.851(8)*						5	2
603.18				8.3(10)			16	5
g 622.79	0.779(29)*	0.867(25)*	0.284(33)*	0.561(27)*		1.03(4)*	33	13
641.20 en	0.85(14)	2.3(4)					40	18
648.31	0.95(9)					11.5(7)	24	8
658.83 n		6.3(6)					10	3
g 675.01	0.722(24)*	0.312(21)*		5.45(17)*			18	5
678.61	0.81(6)		14.9(5)				14	4
699.25 en	0.91(13)	5.8(3)					12	3
g 703.39 d	4.2(8)	8.8(16)					13	3
d	1.093(21)*						6	2
712.82 n	0.86(11)			5.56(30)			19	5
715.19 n			14.3(10)				15	4
722.00			17(3)					
g 730.95				0.765(4)*				
g 738.69 en	0.95(4)*					11.8(4)*	29	8
750.06 n				6.1(12)			20	5
752.59 en					12.3(26)		29	7
g 764.89	1.046(14)*						7	2
g 778.9045	0.958(13)*						8	2
792.56						11.6(27)	32	8
g 794.73	0.89(4)*		16.0(5)*				17	4
g 812.80	1.04(5)*		3.75(28)*				40	14
g 814.38 d			17.7(24)				67	32

d							29	6
818.25 nd	1.1(4)					12(4)	33	8
d							37	12
831.94					13.4(16)			
839.6		28(8)						
841.10 n				5.9(8)			24	5
850.49 n			12.6(22)				18	4
g 855.00 t	0.48(9)	0.65(23)*	3.6(7)	0.89(20)*			15	3
t							25	5
t							38	12
878.13				3.9(9)			27	5
g 893.34 en	0.852(17)*	1.015(20)*		0.32(3)*			33	6
902.46	0.38(4)				14.3(11)		35	7
g 909.15	0.79(4)*			5.1(6)*			28	5
914.35 en	0.77(12)						59	19
g 928.43	0.75(3)	0.87(5)		0.56(11)			40	13
g 932.09	0.89(11)*	0.32(6)*		3.98(19)*			40	12
937.04	1.00(6)		16.8(7)				21	4
953.07 n	0.71(14)						44	12
g 970.32	0.92(10)*						12	2
g 974.05	1.00(4)*						13	2
984.90 en	0.35(12)						45	12
g 990.19	0.820(23)*	4.73(25)*					18	3
993.14	0.83(15)							
1010.60	0.86(3)	0.44(5)		6.18(29)			33	5
1016.60 n	0.96(11)		8.0(9)				71	23
1027.16 en		47(6)					66	21
g1036.74 en	0.92(6)*		2.0(4)*				67	21
g1052.15	0.81(9)*		14.7(5)*				26	4
g1069.15	0.75(11)*							
1075.87 n	0.68(19)						103	42
g1083.96 d	1.03(22)		10.4(13)				28	4
d							49	13
1085.68 n	1.05(17)						67	19
g1089.737 en	1.03(6)*						14	2
1092.26					15(4)		39	7
1106.59 n	0.85(4)		14.1(7)				30	4
1117.15 n	1.4(4)						58	14
g1130.98	1.12(5)*							
g1137.56	0.509(12)*		0.36(6)		13.7(3)*		40	7
1141.68						11.3(21)	42	8
1148.99					20(3)		41	7
g1159.82	0.84(4)*		15.9(6)*				31	4
1185.73	1.11(7)		15.9(7)				33	4
g1190.44	0.59(7)*				13.5(6)		45	7
g1202.64 d						4.0(6)*	37	5

d							46	8
g1205.83 en	0.76(10)*						17	2
g1209.03	0.49(10)*						54	12
1235.57	1.64(29)						77	21
1247.07 n	0.91(8)	1.41(16)	7.9(6)	2.4(3)			55	11
1253.48	1.2(4)							
g1261.32	0.955(22)*							
1263.84 n	1.2(3)			2.9(5)		15.4(21)	48	8
1271.318				4.3(9)				
1275.04 en	0.81(10)	1.38(21)		1.17(22)			74	18
1278.33	0.95(24)							
1284.42 n	0.70(10)						77	19
g1299.140 en	0.990(19)*						19	2
1314.66 d						0.54(5)	12	1
d							50	8
g1316.32	0.180(12)	420(59)		1330(59)			40	5
g1325.86	0.843(22)*	4.84(10)*					33	3
g1336.54	1.07(17)*							
g1348.15 en	1.058(16)*						21	2
1352.98 n	0.67(12)						63	12
1360.43 en		8.2(18)					34	3
1365.69 n	1.00(17)		19.0(13)				36	4
1369.04	0.83(12)			5.8(5)			45	5
1372.04 en	1.2(3)					14.2(20)	52	8
1393.86	1.26(26)			2.8(5)			83	18
g1400.60 d	0.92(11)*			1.04(15)		6.9(8)*	54	8
d							66	13
1406.16	1.09(10)					14.4(10)	55	8
g1411.48 d	1.305(28)*	0.50(5)*		0.44(19)*		1.8(5)	23	2
d							67	13
1417.18						26(5)	56	8
1420.76						12.0(18)	57	8
g1427.32	0.61(7)*						24	2
1430.76 n	0.53(8)	0.55(12)					70	13
1434.54 (n)						5.9(13)	59	8
1441.91 n	0.44(8)				11.6(13)		58	7
g1446.43 d	0.97(5)*		8(5)*				39	4
d							74	14
1481.18 n	0.52(12)					10.3(10)	61	8
1489.60					12.6(24)		60	7
1491.62 n			27(5)				40	4
g1495.44 en	0.73(6)*						28	2
1502.62 n			14.8(29)				41	4
1506.90 n				6.7(8)			50	5
g1517.78 ent	0.97(9)*						30	2
t						2.02(15)	62	8

t							37	3
1544.29						9.6(13)	63	8
g1562.45 n	0.93(10)	0.60(11)*	2.8(6)				74	13
g1565.97	0.40(6)*							
g1571.25	1.04(10)		2.2(4)					
1575.30			18.2(15)				47	4
g1586.22	1.072(23)*		1.32(14)*			13.8(3)	65	8
1593.37 en				4.8(4)			54	5
g1596.75 d	1.40(7)						33	2
d						4.3(3)	66	8
1598.90				6.12(28)*			55	5
g1605.72 d	0.364(17)					5.21(26)	67	8
d							18	1
g1631.42 d	0.93(8)*						34	2
d		4.13(25)					40	3
1640.08 en	0.55(11)				7.1(12)		70	7
1645.92 (en)	0.82(10)						80	13
1663.67					13(3)		71	7
g1667.38 en	0.960(28)*						35	2
1711.02 n				6.2(6)			62	5
1727.72 en	0.80(11)						87	12
1737.03 n				8.0(8)			63	5
g1739.46 n	1.34(8)*					8.1(14)	72	8
g1757.42	1.07(5)*		1.12(7)*	0.23(5)		12.3(3)*	74	8
1761.22 n	1.29(22)5			3.9(7)			90	13
1771.43	0.68(4)				15.2(9)		74	7
1778.78 en	1.00(16)			6.9(6)			65	5
1785.15 n			10.9(14)				56	4
g1789.20 end	0.868(27)*			1.04(7)*			37	2
d							66	5
1792.71					15.7(27)		89	11
1796.83 n						12.9(19)	76	8
g1798.45 n	1.25(14)			7.9(8)			67	5
1802.67 n			14.3(15)				59	4
1809.53 n	1.11(29)					17(4)	79	8
1818.56 n	0.51(14)				14.2(19)		77	7
g1825.37	1.02(7)*						38	2
g1841.15 d	0.94(15)*			2.2(4)		8.9(3)*	71	5
d							80	8
g1857.48 en	1.09(9)*						35	2
g1861.94								
1886.08 n	1.2(3)					15.7(25)	85	8
g1902.45 end	1.072(19)*						40	2
d							86	7
1914.71	0.99(18)							
g1921.00	0.965(28)*						43	2

1932.94					15(3)		87	7
g1941.23								
g1955.36 en	0.970(28)*						45	2
g1970.49								
g1975.65								
g1983.41	0.93(13)*							
1993.87	1.13(13)		23.8(13)				70	4
2018.09			32(5)					
g2033.89	0.75(4)*			6.5(3)*			80	5
g2043.65 d	0.84(10)*				4.7(4)*		48	2
d							98	7
2051.26	1.5(4)			7.7(12)				
2058.47 n	1.35(26)			3.2(8)			82	5
2069.00 n	1.12(19)			6.9(5)			83	5
2076.21		2.5(3)		3.0(7)			84	5
2078.63				5.4(8)			85	5
g2093.51 nd	0.97(17)*	2.07(19)*					50	2
d							65	3
g2103.54 d		2.7(3)					51	2
d							66	3
g2113.70	0.68(10)*	3.9(11)*					67	3
2118.66 n		5.5(5)					68	3
g2150.85 en	1.04(10)*						52	2
2162.05						9.6(23)	102	8
2158.72	1.17(15)		14.9(10)				75	4
g2169.16 d	0.68(17)*			108(14)			53	2
d							92	5
2172.45 n			18.6(23)				77	4
2176.44			8.4(15)					
g2179.42	1.14(9)*						54	2
2182.10 n				4.2(7)			95	5
g2185.24 en	1.17(6)*						55	2
g2196.20	1.14(14)*						56	2
2217.40 n	0.93(15)		2.9(8)			14.1(18)	103	8
2223.71	1.37(27)							
2226.01			17(4)				81	4
g2251.41	1.5(5)*		16.9(4)*				84	4
g2254.54 en	0.77(17)*						60	2
2257.22			17(3)				86	4
2265.33	0.51(12)	4.2(4)					74	3
2306.15 n	0.85(22)			7.4(11)			101	5
2312.00 n	5(3)		17(6)				88	4
2317.61 n		13(4)					79	3
2324.32 n			9.8(15)				90	4
g2342.57	0.93(12)*						64	2
2347.53	1.29(24)							

2350.30 n			16.4(29)				93	4
g2365.13 en	1.17(29)*						65	2
g2375.34	1.146(25)*						66	2
2382.27			25(4)					
2384.94 en	0.96(10)						67	2
2388.72 n			20(3)				97	4
2398.53	1.72(22)		6.9(10)					
g2405.00 en	1.205(21)*						70	2
g2428.36	1.04(11)*							
2479.26			37(9)					
2495.53 n	0.31(6)	10(5)					94	3
d?			6.2(10)					
g2518.42 en	1.52(6)*						72	2
2536.30 en	0.88(3)						74	2
2551.48	0.67(22)							

notes : g – energy of gate transition,

n – new transition,

en – before placed by means of energy balance [5],

* – averaged value from both gates.

Table 10. Decay scheme of ^{152}Tb.

No	E_i, keV	I^π	I_β %	log ft	E_γ keV	XL	E_f keV
1	0.000	0^+	29.9(19)	7.53			
2	344.280(2)	2^+	13.3(17)	7.75	344.279	E2	0.0
3	615.373(18)	0^+	6.8(3)	7.95	615.6	E0	0.0
					271.09	E2	344.280
4	755.395(2)	4^+	0.39(9)	9.29	411.1165	E2	344.280
5	930.550(13)	2^+	7.9(3)	7.80	930.58	E2,M1	0.000
					586.27	M1(E0)	344.280
					315.16	E2(M1)	615.373
					175.14	M1	755.395
6	1047.774(27)	0^+	1.39(9)	8.53	1047.9	E0	0.000

					703.494	E2	344.280
					432.5	E0	615.373
					117.25	E2	930.550
7	1109.193(15)	2^+	2.78(12)	8.21	1109.20	E2,M1	0.000
					764.89	E2,M1	344.280
					493.81		615.373
					353.78		755.395
					178.58	E2,M1	930.550
8	1123.183(4)	3^-	1.66(14)	8.45	778.9045	E1	344.280
					367.80	E1	755.395
9	1227.37(8)	6^+	<0.005	>10.9	471.98		755.395
10	1274.25(8)	2^+	<0.009	>11.4	658.83		615.373
11	1282.267(28)	4^+	0.232(15)	9.22	526.85	E0+M1	755.395
					351.73	E2	930.550
					159.16		1123.183
12	1314.635(20)	1^-	0.69(5)	8.81	1314.635	(E1)	0.000
					970.32	E1	344.280
					699.25		615.373
13	1318.349(17)	2^+	2.89((13)	8.12	1318.24		0.000
					974.05	M1	344.280
					702.976	E2	615.373
					562.98		755.395
					387.80	E0+M1	930.550
					209.14	M1(E0)	1109.193
					195.17	E1	1123.183
14	1434.017(8)	3^+	0.75(4)	8.66	1089.737	E2,M1	344.280
					678.61	E2(M1)	755.395

					503.43		930.550
					324.90		1109.193
15	1470.61(5)	2^+	<0.019	>8.66	855.237		615.373
					715.19		755.395
16	1533.91(11)		<0.003	>11.7	603.18		930.550
17	1550.15(4)	$2^+,3,4^+$	0.287(11)	9.04	1205.83	E1(E2)	344.280
					794.73		755.395
					441.02		1109.193
18	1605.584(18)	2^+	2.30(8)	8.12	1605.584	E1(E2)	0.000
					1261.32	M1	344.280
					990.19	E2	615.373
					850.49		755.395
					675.01	E2	930.550
					557.810		1047.774
					496.37	E0+M1	1109.193
					482.34		1123.183
19	1643.427(13)	2^-	1.85(7)	8.19	1299.140	E1	344.280
					712.82		930.550
					534.21		1109.193
					520.30		1123.183
20	1680.76(5)		0.167(6)	9.18	1336.54		344.280
					750.06		930.550
					366.15		1314.635
21	1692.42(3)	3^+	0.67(3)	8.59	1348.15	E2	344.280
					937.04		755.395
22	1734.44(16)		0.026(2)	10.0	979.04		755.395

23	1755.76(7)	$1^-,2^-,3^-$	0.38(3)	8.91	1411.48	E1	344.280
24	1771.557(26)	2^+	0.343(12)	8.88	1427.32		344.280
					841.10		930.550
					723.67		1047.774
					648.31		1123.183
					489.59		1282.267
					456.92		1314.635
25	1785.24(11)	2^+	0.043(6)	9.78	854.69	E0+M1	930.550
					662.02		1123.183
26	1807.53(5)		0.105(4)	9.88	1052.15		755.395
27	1808.95(8)		0.062(4)	9.60	878.13		930.550
					490.66		1318.349
28	1839.70(4)	2^+	0.267(17)	8.98	1495.44	E0+M1	344.280
					1084.305		755.395
					909.150		930.550
					557.433	M1(E2)	1282.267
29	1861.897(28)	2^+	0.99(3)	8.38	1861.94	E2,M1	0.000
					814.123		1047.774
					752.59		1109.193
					738.69		1123.183
					579.63		1282.267
					543.58	(E0M1)	1318.349
					427.85		1434.017
					218.42		1643.427
30	1862.06(4)	2^+	0.96(5)	8.39	1517.780	M1	344.280
					1106.59		755.395
					547.47		1314.635

31	1915.19(4)	4^+,5,6^+	0.179(12)	9.10	1159.82		755.395
					687.62		1227.374
32	1915.69(4)	2^+,3,4^+	0.156(7)	9.16	1571.25		344.280
					792.56		1123.183
					633.60		1282.267
					597.57		1318.349
33	1941.157(18)	2^+	4.25(14)	7.71	1941.23	(E2)	0.000
					1596.877	E1,E2	344.280
					1325.86	E2(M1)	615.373
					1185.73	E2(E1)	755.395
					1010.60	M1	930.550
					893.34	(M1)	1047.774
					831.94		1109.193
					817.974		1123.183
					622.79	E2,M1	1318.349
					390.82		1550.150
					335.56		1605.584
					298.06		1643.427
					248.75		1692.417
34	1975.67(5)	1^+,2^+	0.174(8)	9.04	1975.65		0.000
					1631.390	E2,M1	344.280
					1360.43		615.373
35	2011.65(4)	1^+,2^+,3^+	0.82(3)	8.40	1667.380	M1	344.280
					902.46		1109.193
					697.20		1314.635
					693.13		1318.349
					577.57		1434.017
36	2120.96(10)	2^+,3,4^+	0.091(5)	9.24	1776.3		344.280
					1365.69		755.395
					839.6		1282.267

37	2133.39(10)	$1^+,2^+$	0.530(24)	8.53	1789.110	E2,M1	344.280
					1518.017		615.373
					1202.84		930.550
					818.755		1314.635
38	2169.58(6)	$1,2^+$	0.144(8)	9.05	1825.37		344.280
					1554.04		615.373
					854.945		1314.635
39	2201.73(5)	2^+	0.292(13)	8.76	2201.65		0.000
					1857.48	E2,M1	344.280
					1446.335	E2(M1)	755.395
					1092.26		1109.193
40	2246.772(23)	2^+	3.74(13)	7.63	1902.492	M1	344.280
					1631.399	E2,M1	615.373
					1491.62		755.395
					1316.32		930.550
					1137.56	M1	1109.193
					932.09		1314.635
					928.43	E2,M1	1318.349
					812.80		1434.017
					641.20		1605.584
					407.12		1839.704
41	2258.14(6)	$2^+,3,4^+$	0.091(6)	9.23	1502.62		755.395
					1148.99		1109.193
					939.84		1318.349
42	2264.83(7)	$1^-,2,3^-$	0.013(5)	10.1	1141.68		1123.183
					950.34		1314.635
					947.08		1318.349
43	2265.28(9)	$1^+,2^+,3^+$	0.42(5)	8.57	1921.00	M1(E2)	344.280

44	2267.71(8)		0.067(3)	9.36	1040.6		1227.374
					953.07	M1	1314.635
45	2299.636(26)	2^+	0.99(3)	8.17	1955.36	E1(E2)	344.280
					1369.04	M1	930.550
					1190.44		1109.193
					1176.53		1123.183
					984.90		1314.635
					865.62		1434.017
					656.42		1643.427
46	2325.82(9)		<0.003	>10.7	1202.64		1123.183
47	2330.70(8)	$2^+,3,4^+$	0.064(3)	9.35	1986.8		344.280
					1575.30		755.395
48	2386.95(11)	$1^-,2,3^-$	0.159(8)	8.92	2042.67		344.280
					1263.84		1123.183
					1072.16		1314.635
49	2401.49(6)	$1^+,2,3^-$	0.201(11)	8.81	1087.12		1314.635
					1083.141		1318.349
					708.98		1692.417
50	2437.44(6)	$1^+,2^+$	0.42(4)	8.47	2437.11		0.000
					2093.16	(M1)	344.280
					1506.90	M1	930.550
					1314.257	E1	1123.183
51	2447.82(12)		<0.018	9.83	2103.54	E2(M1)	344.280
52	2495.17(5)	$1^+,2^+,3^+$	0.272(10)	8.63	2150.85	M1(E2)	344.280
					1372.04		1123.183

53	2513.9(3)	$1^+,2^+$	0.045(12)	9.40	2513.9		0.000
					2169.16	E2,M1	344.280
54	2523.80(4)	2^+	0.676(24)	8.21	2523.92	M1(E2)	0.000
					2179.42	M1	344.280
					1593.370		930.550
					1400.617		1123.183
					1209.03	E1	1314.635
					880.29		1643.427
					684.12		1839.704
55	2529.39(3)		0.183(7)	8.20	2185.24	E2,M1	344.280
					1598.90		930.550
					1406.16	E2(E1)	1123.183
					1247.07		1282.267
					722.00		1807.533
56	2540.45(6)	$2^+,3^+$	0.183(7)	8.77	2196.20	M1	344.280
					1785.15		755.395
					1417.18		1123.183
					1221.95		1318.349
57	2544.00(7)		0.107(4)	9.00	1613.53		930.550
					1420.76		1123.183
58	2551.12(6)		0.139(5)	8.88	1441.91		1109.193
					1117.15		1434.017
59	2557.84(4)	2^+	0.172(6)	8.79	2557.91		0.000
					2211.7	(E0+M1)	344.280
					1802.67		755.395
					1434.54		1123.183
					914.35		1643.427
60	2598.78(5)	$1^+,2^+$	0.289(10)	8.64	2254.54	E2,M1	344.280

					1983.41		615.373
					1489.60	M1(E2)	1109.193
					993.14		1605.584
61	2604.33(5)	1^-,2,3^-	0.158(6)	8.79	2260.05		344.280
					1481.18		1123.183
					1289.64		1314.635
62	2641.56(7)		0.132(9)	8.85	1711.02		930.550
					1518.377	E2,M1	1123.183
63	2667.54(6)	1^-	0.131(6)	8.83	1737.03		930.550
					1544.29		1123.183
					1352.98	E0+M1	1314.635
64	2686.85(10)	1^+,2^+,3^+	0.129(10)	8.83	2342.57	M1(E0)	344.280
65	2709.42(3)	2^+	1.64(6)	7.69	2709.47	E1(E2)	0.000
					2365.13	E0+M1	344.280
					2094.047		615.373
					1778.78	M1	930.550
					1586.22	E1	1123.183
					1066.23		1643.427
66	2719.67(4)	2^+	1.38(5)	7.77	2719.61	E1,E2	0.000
					2375.34	M1	344.280
					2104.297	E2(M1)	615.373
					1789.120	E2,M1	930.550
					1596.487	E1,E2	1123.183
					1401.321		1318.349
					1027.16		1692.417
					454.82		2264.833
67	2729.165(29)	2^+	1.02(4)	7.90	2729.25		0.000
					2384.94	M1(E0)	344.280

					2113.70	M1(E2)	615.373
					1798.45	E2,M1	930.550
					1681.53		1047.774
					1605.982	E1(E2)	1123.183
					1410.816	E2,M1	1318.349
					1258.45		1470.612
					1085.68		1643.427
					1036.74		1692.417
					813.475		1915.191
68	2734.04(7)	1^+	0.145(5)	8.74	2734.06	E1(E2)	0.000
					2118.66	M1	615.373
69	2744.05(11)	1^-	0.084(3)	8.97	2744.10	E1	0.000
					1634.0		1109.193
70	2749.20(3)	$2^+,3^+$	1.58(6)	7.69	2405.00	E1(E2)	344.280
					1993.87		755.395
					1640.08	M1	1109.193
					1475.04		1274.256
					1430.76		1318.349
					1215.20		1533.918
					1056.79		1692.417
					301.82		2448.009
71	2772.36(6)	2^+	0.287(12)	8.42	2772.44		0.000
					1841.810	E2,M1	930.550
					1663.67	E0+M1	1109.193
					1454.08		1318.349
					1338.5		1434.017
					1128.65		1643.427
					1016.60		1755.730
					857.33	(E0M1)	1915.191
72	2862.64(5)		0.231(8)	8.42	2518.42	M1(E2)	344.280

					1739.46	M1(?)	1123.183
					1547.95		1314.635
73	2869.76(10)	$1,2^+$	0.064(10)	9.00	2525.43		344.280
					2254.44		615.379
74	2880.652(21)	$1^+,2^+$	1.82(6)	7.53	2536.30	M1	344.280
					2265.33		615.373
					1771.43	M1	1109.193
					1757.42	(E1)	1123.183
					1565.97		1314.635
					1562.45	M1	1318.349
					1446.635	E2(M1)	1434.017
					1275.04		1605.584
					1188.37		1692.417
					868.94		2011.650
					747.29		2133.395
75	2914.15(7)	2^+	0.250(9)	8.40	2914.42	(M1)	0.000
					2569.85	(E1E2)	344.280
					2158.72	E2(M1)	755.395
					998.37		1915.687
76	2920.08(14)		0.103(5)	8.75	2575.82		344.280
					1811.33		1109.193
					1796.83		1123.183
					1004.2		1915.687
77	2927.85(5)	$2^+,3^+$	0.264(10)	8.33	2583.0		344.280
					2172.45		755.395
					1818.56	M1	1109.193
					1457.25		1470.612
					1284.42		1643.427
					1235.57		1692.417

78	2928.68(24)		0.071(6)	8.90	2584.89		344.280
					1610.11		1318.349
79	2932.66(6)	2^+	0.448(16)	8.10	2588.36	(M1)	344.280
					2317.61		615.373
					1809.53		1123.183
80	2964.33(4)	2^-,3^-	0.334(13)	8.21	2033.89	E1	930.550
					1841.147	E2,M1	1123.183
					1645.92		1318.349
					1530.07		1434.017
					1414.40		1550.150
					1155.48		1808.950
					638.35		2325.928
81	2981.38(9)	2^+,3,4^+	0.054(2)	8.97	2636.93		344.280
					2226.01		755.395
					860.84		2121.061
82	2989.02(9)		0.039(5)	9.10	2644.74		344.280
					2058.47		930.550
					1714.65		1274.256
					1047.9		1941.157
83	2999.52(4)	1^+,2^+	0.233(8)	8.32	2999.69		0.000
					2655.29	E2,M1	344.280
					2069.00	M1(E2)	930.550
					1393.86		1605.584
					829.57		2169.583
84	3006.71(4)	2^+	0.365(13)	8.17	3006.63		0.000
					2662.55	E1,E2	344.280
					2251.41		755.395
					2076.21	E2,M1	930.550
					1732.42		1274.256

					1363.39		1643.427
					1167.0		1839.704
					837.08		2169.583
85	3009.16(6)	$2^-,3^-$	0.120(5)	8.60	2665.18		344.280
					2078.63		930.550
					1886.08	M1(E0)	1123.183
					1694.60		1314.635
					1690.68		1318.349
					1253.48		1755.730
86	3012.06(13)	$2^+,3^+$	0.065(4)	8.86	2668.13		344.280
					2257.22		755.395
					1902.867	M1	1109.193
					1096.60		1915.687
					1000.41		2011.650
					810.44		2201.728
87	3042.30(5)	$0^+,1^+,2^+$	0.329(11)	8.13	2697.99	E2,M1	344.280
					1932.94	M1(E2)	1109.193
					1727.72		1314.635
					1436.67		1605.584
88	3067.40(11)		0.033(2)	9.11	2312.00		755.395
					1944.8	(E0M1)	1123.183
89	3074.86(16)		0.066(4)	8.68	1965.42		1109.193
					1792.71		1282.267
90	3079.64(18)	$3^+,4^+$	0.091(5)	8.60	2324.32	M1(E0)	755.395
					1761.22	E2(E1)	1318.349
91	3090.40(22)		0.009(1)	9.65	2335.00		755.395
92	3098.99(8)		0.156(14)	8.33	2754.70	E2,M1	344.280

					2168.44		930.550
					500.23		2598.784
93	3105.49(7)	2^+	0.057(2)	8.96	3105.45		0.000
					2761.15		344.280
					2350.30		755.395
					805.84		2299.636
94	3110.90(10)	1^+,(2^+)	0.087(3)	8.64	2495.53	M1(E2)	615.373
95	3112.50(8)	1^+,2^+	0.120(8)	8.47	3112.27		0.000
					2768.27		344.280
					2182.10	M1	930.550
					1171.19		1941.157
					583.00		2529.395
96	3140.17(7)	1^+,2^+	0.143(6)	8.39	3140.20		0.000
					2795.92	E2	344.280
					2209.71		930.550
					1198.97		1941.157
					874.85		2264.833
97	3143.96(8)		0.060(2)	8.77	2799.81		344.280
					2388.72		755.395
					2020.67	E2,M1	1123.183
					1022.73		2121.061
98	3152.98(9)	2^+,3,4^+	0.056(10)	8.66	2808.61	E1(E2)	344.280
					2043.787	(E2M1)	1109.210
					1870.55		1282.250
99	3214.23(9)		0.058(3)	8.55	1521.57		1692.417
					1045.31		2169.583
					887.32		2325.928

100	3232.05(9)		0.068(3)	8.61	2887.52	E2,M1	344.280
					2004.93		1227.374
					1917.55		1314.635
					1626.39		1605.584
101	3236.92(9)	2^+,3,4^+	0.073(3)	8.58	2481.75		755.395
					2306.15		930.550
					911.73		2325.928
					788.88		2448.009
102	3285.12(7)	2^+	0.164(7)	8.14	2940.15	E2,M1	344.280
					2162.05		1123.183
					1970.49		1314.635
					1343.0	(E0M1)	1941.157
103	3340.60(5)	3^-	0.118(6)	8.03	2996.26		344.280
					2217.40	M1	1123.183
					1424.76		1915.687
					1075.87		2264.833
104	3358.26(10)	2^+	0.074(10)	10.48	2602.85	E2,M1	755.400
					2043.625		1314.630

References

[1] J.B.Adam, J.J.Adam, M.Honusek, V.G.Kalinnikov, V.S.Pronskikh In: Proceedings of 48 Conference on Nuclear Spectroscopy and Structure of Atomic Nuclei, Moscow, 16-19 June, 1998, p.318.

[2] Krane K.S., Nucl. Instr. and Meth. 98 (1972) 205

[3] D.Venos, private communication.

[4] H.W.Taylor, B.Singh, F.S.Prato, R.McPherson Nuclear Data Tables A9 (1971) 1-83.

[5] D.R. Zolnowski et al. Nuclear Physics A177 (1971) 513.

[6] W.Bambynek et al. Rev.Mod.Phys., Vol.49,No.1, January 1977.

[7] Dzhelepov, B.S., Zyryanova, L.N., and Suslov, Yu.P, 1972, Beta Processes, Functions for the Analysis of Beta-Spectra and Electron Capture (Nauka, Leningrad).

[8] R.B.Firestone, V.S.Shirley, Eds., Table of Isotopes, 8-th Edition: 1998 Update, J.Wiley and Sons, N.Y., 1998.

Received by Publishing Department
on July 25, 2001.

Адам И. и др.
E6-2001-154

Измерения γγ-совпадений и схема распада $^{152}Tb \rightarrow {}^{152}Gd$

На основе γγ-совпадений, регистрировавшихся двумя HPGe-детекторами, в схеме распада $^{152}Tb \rightarrow {}^{152}Gd$ было размещено 242 перехода, из них 131 — впервые. Также впервые было введено 46 новых уровней (всего 111). Для ряда низколежащих уровней получено отношение интенсивностей электронного захвата к позитронному распаду. Для большинства уровней были определены спины и четности, а также log *ft* для заселяющих их распадов.

Работа выполнена в Лаборатории ядерных проблем им. В.П.Джелепова ОИЯИ.

Сообщение Объединенного института ядерных исследований. Дубна, 2001

Adam J. et al.
E6-2001-154

Measurement of γγ-Coincidences
and $^{152}Tb \rightarrow {}^{152}Gd$ Decay Scheme

On the basis of γγ-coincidences recorded with two HPGe-detectors, 242 transitions were placed into the $^{152}Tb \rightarrow {}^{152}Gd$ decay scheme, 131 of them — for the first time. Also, 46 new levels were introduced for the first time (out of 111). For a number of low-lying levels the electron capture to positron decay ratio was found. For the most of levels, their spins and parities were determined, as well as log *ft*'s for feeding them decays.

The investigation has been performed at the Dzhelepov Laboratory of Nuclear Problems, JINR.

Communication of the Joint Institute for Nuclear Research. Dubna, 2001

Макет Т.Е.Попеко

Подписано в печать 17.09.2001
Формат 60 × 90/16. Офсетная печать. Уч.-изд. л. 3,0
Тираж 310. Заказ 52859. Цена 3 р. 60 к.

Издательский отдел Объединенного института ядерных исследований
Дубна Московской области